Biogeosciences Discuss., 10, 10055–10094, 2013
www.biogeosciences-discuss.net/10/10055/2013/
doi:10.5194/bgd-10-10055-2013

Biogeosciences Discussions
Open Access

Partial pressure of CO_2 and CO_2 emission in a monsoon-driven hydroelectric reservoir (Danjiangkou Reservoir), China

S. Y. Li[1,*] **and Q. F. Zhang**[1]

[1]Key Laboratory of Aquatic Botany and Watershed Ecology, Wuhan Botanical Garden, the Chinese Academy of Sciences, Wuhan 430074, China
[*]now at: Southern Cross GeoScience, Southern Cross University, P.O. Box 157, Lismore NSW 2480, Australia

Received: 14 May 2013 – Accepted: 6 June 2013 – Published: 20 June 2013

Correspondence to: S. Y. Li (syli2006@163.com)

Published by Copernicus Publications on behalf of the European Geosciences Union.

Abstract

Hydroelectric reservoirs have been under sampled to establish them as sources or sinks of the atmospheric carbon dioxide (CO_2). Such poor coverage is well known for subtropic, particularly monsoon driven reservoirs in China. Our study presented the spatiotemporal changes of the carbonate system and CO_2 flux in a hydroelectric reservoir (Dangjiankou Reservoir) locating in a subtropical monsoon climate region. Our 21 filed surveys conducted during 2004–2011 revealed significantly spatial and monthly variations of surface water partial pressure of CO_2 (pCO_2) in the Reservoir. pCO_2, showing higher concentrations in the wet and warm seasons, averaged 595 ± 545 µatm (ranging from 53–3751 µatm) in the reservoir surface, while substantially higher pCO_2 (1132 ± 1220 µatm) was observed in the river downstream the dam. A clear pCO_2 drawdown in the reservoir as water flows demonstrated a significantly descending order of Dan Reservoir > site close to dam > Han Reservoir. This spatial contrast can also be seen in the distributions of dissolved inorganic carbon and total alkalinity. Pronounced seasonality in pCO_2 was controlled by seasonal monsoon rainfall, while photosynthetic CO_2 uptake dominated spatial patterns and dry-month variability of pCO_2. We further related pCO_2 to water chemical properties and indicated that pCO_2 had strong positive correlations with Si, TP and DOC, negative correlations with DO saturation, TN and Chl *a*, while weak correlations with other variables including biogenic elements. CO_2 flux from the Reservoir surface showed a bottom average of 9 mmol m^{-2} d^{-1} in comparison with other hydroelectric reservoir in China. River downstream the dam had quite high flux of CO_2 (119 mmol m^{-2} d^{-2}), which was intermediate between temperate rivers and compared to global rivers' average. This means that water releasing from reservoir would be an important channel for atmospheric CO_2 sources. The annual CO_2 emission from the Danjiangkou Reservoir was estimated to be 3.4×10^9 mol C. Remarkably spatial and temporal heterogeneities in CO_2 flux from China's hydroelectric reservoirs are urgently included for advancing global models of reservoirs' carbon emissions.

BGD
10, 10055–10094, 2013

1 Introduction

Inland waters including rivers, lakes and reservoirs have been identified as potentially important sources of green house gas (GHG) including methane (CH_4) and carbon dioxide (CO_2) (St. Louis et al., 2000; Cole et al., 2007; Lima et al., 2008; Battin et al., 2009; Tranvik et al., 2009; Aufdenkamp et al., 2011; Barros et al., 2011; Bastviken et al., 2011; Butman and Raymond, 2011; Fearnside and Pueyo, 2012; Li et al., 2012; Chen et al., 2013). Previous studies reported 1.4 Pg C emission estimate per year as CO_2 from freshwaters, higher than the river-borne carbon transport (1 Pg C yr^{-1}) to the ocean (Tranvik et al., 2009; Amiotte Suchet et al., 2003), this estimated CO_2 emission together with CH_4 emission of 103 Tg CH_4 yr^{-1} (0.7 Pg C (CO_2eq) yr^{-1} expressed as CO_2 equivalents (eq)) have balance the terrestrial carbon sink (Bastviken et al., 2011) and thus represent a critical component of global carbon cycling.

Artificial reservoirs especially the traditional clean hydroelectric reservoirs have been increasingly concerned due to their huge contributions to GHG emissions (Giles, 2006; Lima et al., 2008; Fearnside and Pueyo, 2012). Recent researches particularly on the tropic reservoirs demonstrated quite high C emission fluxes via water–air interface (cf. Fearnside et al., 1995, 2005; Richey et al., 2002; Rosa et al., 2004; Dos Santos et al., 2006; Guerin et al., 2006; Kemenes et al., 2007, 2011), and the "green" credentials of hydroelectricity have been quashed (Giles, 2006). For instance hydropower reservoirs such as Samuel, Tres Marias, and Barra Bonita, in the tropic zone posted higher C emission than their equivalent thermo-power counterparts (Dos Santos et al., 2006). These observations cause the doubts on the effects of hydroelectricity on global GHG reduction.

The more recent work by Barros et al. (2011) estimated 48 Tg C as CO_2 and 3 Tg C as CH_4 annually from hydroelectricity, respectively, a downgrade from earlier estimates of 321 Tg C yr^{-1}. The estimate was based on 85 globally distributed hydroelectric reservoirs from the Americas and Northern Europe. No reservoirs from Asia especially from China were included, which could be a key component that limits the C emission quan-

BGD
10, 10055–10094, 2013

tification due to more than 80 000 reservoirs in operation and many projected in China, as reflected by Barros et al. (2011) that carbon fluxes from reservoirs correlate well to reservoir age, size, latitude, and environmental factors. This was corroborated by distinct sample size and incomplete coverage of spatial cases in particular, which contributed to large variability of CO_2 releases from global reservoirs. For example, the areal flux of CO_2 in the temperate reservoirs averaged 387–1400 mg CO_2 m^{-2} d^{-1} (St. Louis et al., 2000; Barros et al., 2011). A broad ranges were also found for CH_4 release from global hydroelectric reservoirs, i.e., from 4 Tg CH_4 yr^{-1} (Barros et al., 2011) to 100 Tg CH_4 yr^{-1} (Lima et al., 2008). Thus, more data particularly in China is urgently fueled for precise assessment on the liberation of GHG from hydroelectric reservoirs.

China, one of the largest hydroelectricity producer has a hydropower capacity of 654×10^9 kWh yr^{-1}, contributing 14 % to the total national electricity. More than 40 000 reservoirs are located in the Yangtze basin with subtropical monsoon climate, while very few reports concern their GHG emissions. Until now, methane efflux has only been studied for the Three Gorges Reservoir (TGR) (Chen et al., 2009, 2011; Yang et al., 2012; Zhao et al., 2013), Miyun (Yang et al., 2011) and Ertan (Zheng et al., 2011), however, more limited studies were conducted on CO_2 emissions from hydropower reservoirs, i.e., two papers from ISI-listed journals (e.g., cascade reservoirs (Hongfeng, Baihua, Xiuwen and Hongyan) in the Wujiang of the Yangtze basin by Wang et al., 2011, as well as TGR by Zhao et al., 2013), and five Chinese journal papers (Hongjiadu by Yu et al., 2008; Xin'anjiang by Yao et al., 2010; Nihe by Lu et al., 2010; Wan'an by Mei et al., 2011; Shuibuya by Zhao et al., 2012, which are not readable by international scholars). Therefore, carbon emission from reservoirs in China largely lags behind. Combining very limited studies with clearly spatial (cf. 10–90 mg CO_2 m^{-2} h^{-1} for) and temporal (cf. −22–330 mg CO_2 m^{-2} h^{-1}) heterogeneities in CO_2 flux relating to China's hydroelectricity, we can urge that current data paucity of carbon release from China's reservoirs is constraining the accurate quantification of global carbon emission from hydroelectric reservoirs.

BGD
10, 10055–10094, 2013

Similar to reservoirs in the tropical zone, Chinese hydroelectric reservoirs also receive world-wide concerns mainly because of very high methane flux ($6.7 \pm 13.3\,mg\,CH_4\,m^{-2}\,h^{-1}$) and CO_2 flux ($88–175\,mmol\,m^{-2}\,d^{-2}$) from the Three Gorges Reservoir (TGR) (Chen et al., 2009; Zhao et al., 2013) and consequently have been described as "GHG menace" reported in Nature News (Qiu, 2009). However, this perspective is challenging by the drastically downward revision of the previous emission rate. For example, the subsequent measurements of 0.29 and $0.18\,mg\,CH_4\,m^{-2}\,h^{-1}$ (Yang et al., 2012), 3–4 % of the previous CH_4 flux in the drawdown area of the TGR (Chen et al., 2011) implied carbon emission from hydroelectricity could be largely over-estimated. Spatiotemporal sampling and varied calculated methods caused large differences in CO_2 flux from monsoonal rivers such as Yangtze and Pearl River systems (Yao et al., 2007; Wang et al., 2011; Li et al., 2012). These could potentially cause an over-estimate of CO_2 flux from TGR, where extremely high level occurs when compared to other China's hydropower reservoirs and is comparable to the tropical reservoirs (e.g., Petit Saut and Balbina) (cf. Zhao et al., 2013; Guerin et al., 2006). Therefore, more cases should be developed to better constrain the GHG emission from China's hydroelectricity

Consequently, our study here focuses on the Danjiangkou Reservoir in the Han River, which belongs to Yangtze drainage basin and has a subtropical monsoon climate. The main objectivities are to (1) examine the spatial and temporal changes of partial pressure CO_2 (pCO_2), (2) unravel the mechanisms controlling the variability of pCO_2 and (3) quantify the water–air interface CO_2 flux in the surface water of the reservoir.

2 Material and methods

2.1 Study area

The Danjiangkou Reservoir (32°36′–33°48′ N, 110°59′–111°49′ E) built in 1970s is situated in the juncture of Hubei and Henan provinces, Central China. It has a drainage

BGD
10, 10055–10094, 2013

area of approx. 95 000 km^2 which includes the upper Han River and Dan River basins (Fig. 1; Li et al., 2008b, 2009a). The Reservoir drains a region of northern subtropical monsoon climate with distinct transitional climatic characteristics. The annual mean temperature is 15–16 °C. The average annual precipitation is 800–1000 mm with large inter and intra-annual variability, and 80 % of which concentrates in the time period of May through October (Li et al., 2009a; Li and Zhang, 2010). Similar to the rainfall patterns, the 41.1 × 10^9 m^3 yr^{-1} runoff from its upper basin to the Reservoir also shows large annual and interannual variability. For example, in the historical records, the flood peak was 34, 300 m^3 s^{-1}, the mean maximum monthly flow was 7500 m^3 s^{-1} in the wet season and the minimum flow in the dry season was 64 m^3 s^{-1} (cf. Li et al., 2009a).

Currently, the water level of the Reservoir is 157 m, and its corresponding water surface area and storage capacity are 745 km^2 and 17.5 × 10^9 m^3, respectively. Due to the China's South to North Water Transfer Project, the water level will be 170 m with the dam height increasing from the current 162 m to 176.6 m, the water surface area will reach 1050 km^2 when the project is finished in 2014. In our study, five sampling sites during 2004–2006 while eight sites for 2007–2011 were geolocated in the Reservoir using a portable Global Position System (Table 1 and Fig. 1).

2.2 Water sampling and analyses

21 field surveys were conducted for water samplings in the Danjiangkou Reservoir during 2004–2011 (Table 2). A total of 432 grab water samples (3 L), consisting of three replicates within a 200 m diameter circle, were taken from 50–100 cm depth below water surface using previously acid-washed high-density polyethylene (HDPE) containers. Thus, a total of 144 samples were pretreated for laboratory analysis after mixing with replicates. The acid-washed containers were rinsed thrice with sampled water on site, and the rinsing process was carried out downwind. A 500 mL subsample was filtered in situ through a previously acid-washed 0.45 µm pore Millipore nitrocellulose membrane filter. The initial portion of the filtration was discarded to clean the membrane.

BGD
10, 10055–10094, 2013

A small portion of the filtrate was used for measuring major anions Cl^-, F^- and SO_4^{2-}, while another portion for major cation analyses was acidified to pH < 2 using ultra-pure concentrated nitric acid. Filtrates for measurements of dissolved organic carbon (DOC), dissolved nitrogen (DN) and solute reactive phosphate (SRP) were also prepared. Raw water samples for determination of total phosphorus (TP), total nitrogen (TN), total organic carbon (TOC), biogeochemical oxygen demand (BOD) and chemical oxygen demand (COD) were acidified with 10 % (v/v) sulphuric acid to pH < 2. Filtrates and raw samples were all stored in pre-cleaned HDPE bottles, and transported to the laboratory in a refrigerator at 4 °C.

Water temperature (T), pH, dissolved oxygen (DO), oxidation-reduction potential (ORP), electrical conductivity (EC), turbidity, nitrate-nitrogen (NO_3^--N) and ammonium-nitrogen (NH_4^--N) were determined on site using a YSI 6920 (YSI Inc., Yellow Springs, Ohio, USA). The instrument was calibrated at 0 and 100 % oxygen saturation before and after usage for DO measurement. The pH electrode was calibrated at 7 and 10, and turbidity electrode at 123 and 0 before sampling. The nitrogen sondes were both calibrated at 100 and 1 mg L^{-1} before sampling. The membranes used for filtration were dried at 63 °C to constant weight, and total suspended solid (TSS) was calculated from the difference in the filter paper weights before and after filtering. Alkalinity, a measurement of bicarbonate buffering components in solution, was determined by titration of hydrochloric acid (0.020 M) in situ to pH 4.5 using Methyl orange (Li and Zhang, 2008, 2009, 2010). Total phosphorus (TP) was analysed with acidified molybdate to form reduced phosphor-molybdenum blue and measured spectrophotometrically at 700 nm, with the method detection limit (MDL) of 0.01 mg L^{-1} (CSEPB, 2002). SRP was determined by the same analytical method as TP, but measured spectrophotometrically at 882 nm (CSEPB, 2002). TN and DN were determined by alkaline potassium persulfate digestion-UV spectrophotometric method, and TOC and DOC were determined using TOC analyzer (MultiN/C2100 TOC/TN, Jena). Chlorophyll *a* (Chl *a*) was analysed using spectrophotometer. Determinations of BOD and COD were following Li et al. (2008a).

BGD
10, 10055–10094, 2013

The methods given by the Chinese State Environment Protection Bureau were followed in all the procedures (CSEPB, 2002).

Anions (Cl^-, F^- and SO_4^{2-}) were measured using a Dionex Ion Chromatograph (Dionex Corporation, Sunnyvale, California, USA). An inductively-coupled plasma optical emission spectrometer (ICP-OES) (IRIS Intrepid II XSP DUO, USA) was used to determine the concentrations of major cations (K^+, Ca^{2+}, Na^+ and Mg^{2+}), Si and dissolved phosphorus. Reagent and procedural blanks were determined in parallel to the sample treatment using identical procedures. Each calibration curve was evaluated by analyses of these quality control standards before, during and after the analyses of a set of samples. Our analytical precision for major cations was better than ±10 %, and ±5 % for major anions.

2.3 pCO_2 calculations

There are direct and indirect methods using acidimetric titrations for pCO_2 determinations. The direct method, named the headspace technique, has been described in detail by Hope et al. (1995). The indirect method, much simplified procedure of alkalinity determination by titration to pH 4.5, has been widely used, i.e., pCO_2 is calculated via pH/DIC and pH/alkalinity in particular (Neal et al., 1998a,b; Telmer and Veizer, 1999; Yao et al., 2007; Butman and Raymond, 2011; Wang et al., 2011; Li et al., 2012). This titration based method for measurements of dissolved CO_2 are well acknowledged especially for natural rivers with pH > 6 and low organic carbon content.

Popular methods for measurements of pCO_2 include temperature-dependent constants in the chemistry equilibrium via pH/alkalinity (commonly used) (i.e., Neal et al., 1998a,b; Telmer and Veizer, 1999; Yao et al., 2007; Wang et al., 2011; Li et al., 2012) and CO_2SYS (Lewis and Wallace, 1998). The former detailed algorithm has been presented elsewhere (i.e., Yao et al., 2007; Wang et al., 2011; Li et al., 2012). The program CO_2SYS dependent on measured pH, alkalinity and water temperature, employed in our work, was considered to be reliable (cf. Hunt et al., 2011; Butman and Raymond, 2011; Sarma et al., 2011).

BGD
10, 10055–10094, 2013

2.4 Water–air interface CO_2 flux calculations

The diffusion flux of CO_2 (F) across the water–air interface can be estimated based on a theoretical diffusion model: $F = k \times K_h \times (pCO_{2water} - pCO_{2air})$.

Where k is the gas transfer velocity of CO_2 (also referred to as piston velocity), pCO_{2water} in µatm is the partial pressure of CO_2 in the surface water, and pCO_{2air} in µatm is the CO_2 concentration in equilibrium with atmosphere. K_h is the solubility of CO_2 corrected using temperature. This model has been widely used (i.e., Telmer and Veizer, 1999; Richey et al., 2002; Yao et al., 2007; Teodoru et al., 2009; Alin et al., 2011; Wang et al., 2011; Li el., 2012).

The piston velocity (k in $cm\,h^{-1}$) of CO_2 at the water–air interface is affected by different basin physical factors but largely by wind speed and water turbulence (Telmer and Veizer, 1999; Alin et al., 2011). Extensive efforts have been made to improve the reliability of k term for highly precise and accurate methods of water–air CO_2 evasion, such as k values from a suit of empirical functions of wind speed (i.e., Wanninkhof, 1992; Raymond and Cole, 2001; Alin et al., 2011). However, k values from their models showed large differences (Zhai et al., 2007).

The riverine k values showed wide ranges of $3\,cm\,h^{-1}$ to $115\,cm\,h^{-1}$ (Aucour et al., 1999; Raymond and Cole, 2001), however, 8–15 $cm\,h^{-1}$ for k values has been widely adopted for large rivers, for instance k values (8–15) in the River Rhone and Saone (Aucour et al., 1999), $10\,cm\,h^{-1}$ for Amazon mainstream (Raymond and Cole, 2001) and $15\,cm\,h^{-1}$ for St Lawrence (Yang et al., 1996). Albeit 8–15 $cm\,h^{-1}$ of k value was designated in Xijiang River and Wujiang River (Yao et al., 2007; Wang et al., 2011), Alin et al. (2011) got the k_{600} level of $22\,cm\,h^{-1}$ at a temperature of 20 °C for Asian monsoon river (e.g., Mekong), and $20\,cm\,h^{-1}$ for temperate rivers (Aufdenkampe et al., 2011). Thus, we estimated an averaged k of $15\,cm\,h^{-1}$ in the river downstream the dam considering the normal k level of $10\,cm\,h^{-1}$ due to the similar hydrographic features with other Yangtze River system and world rivers (Aucour et al., 1999; Yao et al., 2007; Wang et al., 2011), and $20\,cm\,h^{-1}$ for reservoir discharge with high turbulence.

BGD
10, 10055–10094, 2013

Considering the mean wind speed in the Dnajiangkou Reservoir is around 2.5 m s^{-1}, thus, the k level of water surface in the Danjiangkou Reservoir can be calculated using a function of wind speed and temperature (Cole and Caraco, 1998):

$$k_{600} = 2.07 + 0.215U_{10}^{1.7} \quad (1)$$

$$k_{600} = k_T \left(\frac{600}{Sc_{CT}}\right)^{-0.5} \quad (2)$$

$$Sc_{CT} = 1911.1 - 118.11T + 3.4527T^2 - 0.04132T^3 \text{ (Wanninkhof, 1992)} \quad (3)$$

where k_T is the measured values in situ temperature (T), Sc_{CT} is the Schmidt number of temperature T (unit in °C), and U_{10} is the wind speed at 10 m above waters (m s^{-1}). Here, T = 20 °C, Sc_{CT} = 600 and k_{600} = 3.1 cm h^{-1}, which is comparable to other reservoirs in China, i.e., 2–4 for k value (cf. Yao et al., 2010; Mei et al., 2011; Wang et al., 2011). Then we can get the in site temperature-dependent k levels using the Eqs. (2) and (3).

2.5 Statistical analyses

Multivariate statistics such as correlation analyses and analysis of variance (ANOVA) were used in our study. Correlation analyses was employed for relations between pCO_2 and environmental parameters, while ANOVA was performed for differences of spatial and monthly DIC system with significance at $p < 0.05$. The statistical processes were conducted using SPSS 16.0 (Li and Zhang, 2009; Li et al., 2013).

3 Results

3.1 Variability of water temperature, pH and alkalinity

The original data of water temperature (T), pH and alkalinity were presented in Fig. S1. Their descriptive statistics were listed in Tables 2 and 3. T averaged 9 ± 0.4 °C to

BGD
10, 10055–10094, 2013

$29 \pm 1.4\,^{\circ}C$ with minimum and maximum in winter (January 2010) and summer (July 2008), respectively. pH showed lower values in the monsoon rainy season, for example, June through November, ranging from 7.81 ± 0.18 (November 2009) to 8.65 ± 0.09 (January 2010). Alkalinity ranged from 1795 ± 456 (August 2010) to $3241 \pm 332\,\mu mol\,L^{-1}$ (November 2008) (Table 2). In total, water temperature, pH and alkalinity averaged $18.75\,^{\circ}C$, 8.22 and $2385\,\mu mol\,L^{-1}$, respectively and all of them exhibited significant monthly differences ($p < 0.01$ by ANOVA; Table 4a).

Contrary to the monthly variations, T and pH in the Danjiangkou Reservoir showed insignificant variability among sampling sites (Table 4b). T and pH levels in the reservoir surface were higher than the site downstream the dam (DJK5) with lowest averages of $16.4 \pm 8\,^{\circ}C$ for T and 8.01 ± 0.38 for pH (Table 3). However, alkalinity showed significant variations among sites with highest and lowest levels of $2736 \pm 437\,\mu mol\,L^{-1}$ (DJK1 in the Dan Reservoir) and $2117 \pm 390\,\mu mol\,L^{-1}$ (DJK4 in the Han Reservoir), respectively. Generally, alkalinity significantly decreased in the Dan Reservoir as water flows ($R^2 = 0.68$, $p < 0.01$) till the site (DJK 4) in the Han Reservoir, and then increased significantly onward till the downstream of the dam ($R^2 = 0.93$, $p < 0.01$). In total, alkalinity in the different zones of the Reservoir was following in an order of Dan Reservoir > river downstream the Reservoir > site close to dam > Han Reservoir.

3.2 Dissolved inorganic carbon (DIC) species

The DIC species calculated using CO_2SYS were presented in Figs. 2, 3 and 4. HCO_3^-, showing similar trends with DIC in space and month, was the dominant component of DIC for all samples, accounting for ~ 93.5 % of DIC on average, followed by dissolved CO_3^{2-} and CO_2, accounting for 5.3 % and 1.2 %, respectively. Also, HCO_3^- accounted for almost all of the alkalinity, up to an average of 97.4 %.

There were pronounced monthly and spatial variations in pCO_2 illustrated by box-whiskers plots (Figs. 2, 3, and 4). Monthly statistics of pCO_2 in the Reservoir area generally showed same medians and means with the ratio of 0.83–1.17 (median/mean), while extremely spatial variations resulted in that the mean concentration (491 µatm)

BGD
10, 10055–10094, 2013

was three-fold the median (154 µatm) in July 2006 (Fig. 2). Both of them displayed the minimal and maximal concentrations in the flooding season (ca. June–November), i.e., pCO_2 median values ranged 90 µatm in August 2009 to 1530 µatm in November 2008, while 110 (August 2009)–1580 µatm (November 2008) for pCO_2 mean values (Fig. 2).

As for pCO_2 downstream the Reservoir, highest level (4764 µatm) occurred in July, and lowest level (155 µatm) in January 2010 (Fig. 3). pCO_2 concentrations in the site downstream the dam were consistently higher in relation to those in the reservoir surface when November 2008 was excluded (Figs. 2 and 3).

Spatial patterns indicated great variations from 53–3751 µatm and 155–4764 µatm of pCO_2 upstream and downstream the dam, respectively (Fig. 4). The box-whiskers plots illustrated that pCO_2 median levels significantly decreased as water flows in the Dan Reservoir ($R^2 = 0.41$, $p < 0.05$). There was a significant decrease ($R^2 = 0.61$, $p < 0.05$) in terms of pCO_2 medians from Dan Reservoir–Han Reservoir–Dam with lowest level (320 µatm) in the site close to Dam. The maximal median (702 µatm) was observed downstream the dam (Fig. 4).

pCO_2 mean values significantly decreased from the Dan Reservoir to Han Reservoir ($R^2 = 0.42$, $p < 0.05$), then increased quickly till the downstream of dam ($R^2 = 0.88$, $p < 0.05$) with lowest (477 µatm) and highest levels (1132 µatm) in sites D2 (Han Reservoir) and DJK5 (downstream of the dam), respectively. The pCO_2 mean values were consistently higher relative to pCO_2 medians, reflected by the ratio of mean to median from 1.14 (D1 in the Dan Reservoir)–1.87 (D3 close to the dam). Regarding to respective sampling site, large variation factors of pCO_2 (max./min.) varied from 9 at DJK2 in the Dan Reservoir to 31 at the river downstream the Reservoir (Fig. 4). pCO_2 totally averaged 595 ± 545 µatm (mean± S.D) in the reservoir surface area, which was around 1/2 of the average downstream the Reservoir (1132 ± 1220 µatm).

BGD
10, 10055–10094, 2013

3.3 CO_2 diffusion fluxes of the Danjiangkou Reservoir

The average CO_2 diffusion fluxes (FCO_2) were calculated, as illustrated in Fig. 5. FCO_2 was generally higher in the wet season, with averages of −8.2–31.4 mmol m^{-2} d^{-1}, and in the dry season, it ranged from −5.8–10.6 mmol m^{-2} d^{-1} in the reservoir surface waters. Similar to the distribution of pCO_2, FCO_2 demonstrated remarkable variations upstream and downstream the dam in each sampling month. Generally, FCO_2 downstream the dam was quite high, with ranges of −20–703 mmol m^{-2} d^{-1} in the wet season, and −38–125 mmol m^{-2} d^{-1} in the dry season (Fig. 5a).

Spatial FCO_2 in the reservoir surface demonstrated the following descending order: Dan Reservoir (3.2–13.7 mmol m^{-2} d^{-2}) > the site close to dam (6 mmol m^{-2} d^{-2}) > Han Reservoir (3–3.4 mmol m^{-2} d^{-2}) (Fig. 5b). FCO_2 downstream the dam was much higher than the reservoir surface, i.e., averages of 119 vs 9 mmol m^{-2} d^{-1} for downstream and upstream the dam, respectively (Fig. 5). In total, the Danjiangkou Reservoir emitted 2.4×10^9 mol CO_2 yr^{-1} in the current situation while 3.4×10^9 mol CO_2 yr^{-1} from 2014 onward, respectively representing 8.3 % and 11.7 % the CO_2 emission from Three Gorges Reservoir (ca. 29.5×10^9 mol CO_2 yr^{-1}; Zhao et al., 2013).

4 Discussion

4.1 Controls on aqueous pCO_2 (CO_2 flux)

Potential processes such as soil CO_2 by runoff and in situ aquatic respiration of organic carbon would elevate pCO_2 in water, and resulted in oversaturated CO_2 in the rivers worldwide with respect to atmosphere (cf. Cole and Caraco, 2001; Richey et al., 2002; Yao et al., 2007; Sarma et al., 2011; Wang et al., 2007, 2011; Li et al., 2012), albeit photosynthesis and water–air interface CO_2 evasion decrease the aqueous pCO_2 (Cole and Caraco, 2001; Zeng and Masiello, 2010). Temperature and monsoonal precipitation in the upstream of the Danjiangkou Reservoir (Fig. 6) thus have large effects

BGD
10, 10055–10094, 2013

on aquatic pCO_2 levels due to that rainfall alters the biogeochemical processes in the terrestrial ecosystem and organic carbon composition in the Reservoir (Yao et al., 2007; Zeng and Masiello, 2010). This hypothesis was corroborated by pronounced seasonality in pCO_2 concentrations (Figs. 2 and 3). Previous researches reported that negative or positive contributions of rainfall events to pCO_2 depend on rainfall intensity and basin impermeability (Ho et al., 1997; Yao et al., 2007; Zeng and Masiello, 2010; Li et al., 2012), for example, initial rainfall enhances the export of soil CO_2 and soil organic carbon load to river system, while continued rain especially the concentrated precipitation lower soil permeability and consequently shows dominant dilution effects. These mechanisms could explain large variability in pCO_2 occurring in the wet months (ca. August 2005 vs August 2009) (Fig. 2). In the year of 2009, persistent precipitation (22 July to 5 August) and particularly the extreme storm (i.e., 62 mm d^{-1}) from the onset of August (Fig. 6) had flushed out the soil CO_2 and hence storm dilution effects dominated, which resulted in the trough of pCO_2 on 11 August (Fig. 2).

Samplings in 2005 allowed us analyze seasonal controls on pCO_2 in a hydrological year (Fig. 7). Little rainfall occurred between the date of sampling in January and April in 2005, while rise in temperature and algae blooming increased photosynthesis in the Spring season would reduce aquatic pCO_2 (from 372 to294 µatm). From May afterward, more rainfall events occurred due to monsoonal effects, and enhanced pCO_2 in May could be assumed albeit no sampling in May 2005. However, this could be supported by the pCO_2 concentrations observed in May 2007 (582 µatm) and May 2011 (650 µatm), which was likely caused by export of soil CO_2 by rain runoff. Weaker biological CO_2 uptake through photosynthesis due to lower sun angle and high-turbid water might be additional reasons for the rapid pCO_2 increase. The continued rain especially the storm water with lower permeability or without infiltration into soil contributed to the trough of pCO_2 (150 µatm) in June. However, from the late of July to the mid-August, proper temperature and wetted soils by lower precipitation favored soil bacterial respiration and thus higher soil CO_2 content, consequently making elevated aqueous pCO_2 via baseflow and interflow albeit more rainfall events in 13–19 August partially con-

BGD
10, 10055–10094, 2013

tributed to dilution effects. As expected, precipitation showed a quick decrease from the mid-October onward, evenly distributed precipitation and appropriate rainfall, however, provided optimum environment for soil respiration (cf. Zeng and Masiello, 2010; Li et al., 2012). This allowed the rain water to infiltrate and flush out soil CO_2 to the river with limited dilution effects, and therefore contributed to the crest level of pCO_2 in November (Fig. 7), as indicated by other two major pCO_2 peaks in November in 2008 and 2009 (Fig. 2). Henceforth, little rainfall and lowest temperature in December through January limited the export of soil CO_2 to rivers, which resulted in very low pCO_2 in January (the most cold and dry month) (Fig. 7).

Consistent with previous studies (Richey et al., 2002; Yao et al., 2007; Zeng and Masiello, 2010; Li et al., 2012), pCO_2 in the reservoir surface was generally higher in the warm and wet season (May–November) than in cold and dry season (December–April) (Figs. 2 and 7). We also concluded that enhanced photosynthesis due to abundant phytoplankton and high water temperature could not explain clearly pCO_2 fluctuations by a factor of more than 10 in the monsoon season (Fig. 2) (Cole et al., 1992). This was corroborated by previous studies (cf. Zeng and Masiello, 2010) that diurnal pCO_2 showed little changes in the day with little rain while large differences in the rainier day, as well as little differences of diurnal pCO_2 in the Nihe Reservoir, China (Lu et al., 2010).

Different monthly patterns of pCO_2 occurred in the river downstream the Danjiangkou Dam when compared to reservoir surface waters (Fig. 3). This could be responsible for artificial water regulation, for example, water discharges via deep turbines before monsoonal flooding arrival for flood control strategy made the extremepCO_2 in July. However, the second pCO_2 peak level in November 2009 was due to autumn flooding.

As water flows in the reservoir, aquatic ecosystem gradually transformed from "heterotrophy" to "autotrophy" with more photosynthetic uptake of CO_2 close to dam (Saito et al., 2001). This could explain the significant decrease as water flows in the Dan Reservoir ($R^2 = 0.41$, $p < 0.05$ for pCO_2 medians). However, both pCO_2 medians and

BGD
10, 10055–10094, 2013

means were higher in the Dan Reservoir than in the Han Reservoir, which could be contributable to higher pollution load and thus relatively lower pH in the Dan Reservoir zone (Li et al., 2009a). Shifts of hydrological dynamics, nutrient structure and complicated biogeochemical process in the reservoir generally reduced the pCO_2 close to the dam, as indicated by significant decreases in pCO_2 medians from Dan Reservoir–Han Reservoir–Dam ($R^2 = 0.61$, $p < 0.05$; Fig. 4), as well as other cases in China such as Wan'an (Mei et al., 2011) and Xin'anjiang Reservoirs (Yao et al., 2010). Turbines with intake of deep water in the Danjiangkou Reservoir produce a hydroelectricity of 45×10^8 kWh yr^{-1}, this water releases had hypoxic environment with lower pH and higher CO_2 concentration (cf. Wang et al., 2011), as well as considerably enhanced pCO_2 in the river downstream the dam. Similar results were obtained in China's other hydroelectric reservoirs such as Hongjiadu (Yu et al., 2008) and Xin'anjiang (Yao et al., 2010).

4.2 Correlations between water quality and pCO_2

Apart from precipitation prevailing on monthly pCO_2 variations, as well as hydrological and biogeochemical processes on spatial pCO_2 variations in the reservoir area, water chemical variables including nutrients (ammonium-N, nitrate-N, total-N, dissolved N, soluble reactive phosphorus, dissolved phosphorus, total phosphorus (TP), DO%), organic carbon (TOC, DOC), biogenic elements (Cl^-, SO_4^{2-}, Na^+, K^+, Ca^{2+}, Mg^{2+} and Si), water pollution parameters (chemical oxygen demand (COD), biochemical oxygen demand (BOD), total suspended solid (TSS), turbidity) and Chl *a* were correlated to pCO_2 to gain insights of the possible controls (Fig. 8; Table S2). Our data indicated that pCO_2 was significantly and positively related to Si, TP and DOC and negatively to DO saturation, TN and Chl *a*, while slightly to other water variables including biogenic elements.

The increased nitrogen could enhance aquatic photosynthesis and thus O_2 production, while reduce dissolved CO_2 level (e.g., Cole and Caraco, 2011; Wang et al., 2007), which was relevant to the negative relationships between pCO_2 and nitrogen, Chl *a* and

BGD
10, 10055–10094, 2013

DO concentration (Table S2). Higher organic carbon appeared to facilitate high bacteria respiration (cf. Sarma et al., 2009, 2011; Zeng and Masiello, 2010), and thus led to increase in pCO_2, while O_2 was consumed simultaneously. This process was consistent with the algal photosynthesis process that caused opposite changes between pCO_2 and O_2 The results were in excellent agreement with the observations in other China's hydropower reservoirs, e.g., Shuibuya (Zhao et al., 2012), Wan'an (Mei et al., 2011) and Three Gorges Reservoir (Zhao et al., 2011, 2013).

Moreover, aquatic ecosystems tend to have an optimum nutrient stoichiometry of phytoplankton (e.g., Redfield Ratio; Redfield, 1958). Phytoplankton via photosynthesis assimilates dissolved CO_2 and nutrients such as nitrogen, phosphorus, and silica in a stable element stoichiometric ratio. Thus, dramatic increase in nitrogen load due to anthropogenic inputs in the upper basin of the reservoir (Li et al., 2009b, 2013) could stimulate the assimilation of dissolved CO_2 and P and Si by aquatic photosynthesis. Slightly increase in P and exclusive source from silicate weathering for Si in the upper Han River (Li et al., 2009c) understandably resulted in positive correlations between pCO_2 and Si and P. These trends were, in general, in concurrence with the results elsewhere (cf. Wang et al., 2007). Yet these processes could not explain the associations between pCO_2 and nitrogen species and biogenic elements, this could be attributed to multi-collinear effects of water quality properties, for example, varied effects of nitrate on pCO_2 were observed (cf. Wang et al., 2007; Li et al., 2012).

4.3 Comparison with other water areas

CO_2 efflux (9 mmol m^{-2} d^{-2}) from the Danjiangkou Reservoir surface area was at the bottom in contrast to other China's hydroelectric reservoirs (e.g., 6–96 mmol m^{-2} d^{-2}), which resulted in that total CO_2 emission from the Danjiangkou was an order of magnitude lower than the TGR albeit they have same water surface area (Zhao et al., 2013). Our estimated CO_2 emission rate was much higher than some temperate reservoirs (e.g., Wallula, New Melones and Dworkshak): these three reservoirs acted as the atmospheric CO_2 sink, however, much lower than those from boreal and tropic reser-

BGD
10, 10055–10094, 2013

voirs. For example, the estimate of CO_2 flux was around 40 % of that from Arrow-Upper (boreal) and only 1 % that from Samuel (tropic) (see Table 5).

On the basis of the available literature, Barros et al. (2011) recently estimated an average of CO_2 flux $\sim 8.8\,mmol\,m^{-2}\,d^{-1}$ from temperate hydroelectric reservoirs (25–50° latitudinal belt). Our calculated CO_2 flux from the Danjiangkou Reservoir equaled to the currently estimated global average for the mid-latitude reservoirs, however, there exited significantly geographical heterogeneities in CO_2 flux from China's hydroelectric reservoirs (see Table 5). For the global estimates, data on CO_2 emission China's reservoirs have been excluded (cf. St Louis et al., 2000; McCully, 2006; Aufdenkampe et al., 2011; Barros et al., 2011). This indicated that the current global estimation of CO_2 emission from reservoirs could be under-estimated or overestimated, as reflected by the wide ranges (see Table 5). It is clear therefore that more data particularly in China, where a large number of hydropower dams exist with many planned for the future, are mandatory to better constrain the global CO_2 emission from hydroelectric reservoirs.

Worldwide riverine pCO_2 was primarily 2–20 times supersaturated in CO_2 relative to the atmosphere (Cole and Caraco, 2001), our calculations of 1132 ± 1220 µatm (ranges of 155–4764 µatm) in the river downstream of the Reservoir was three times lower than global river's average (3230 µatm calculated from world 47 large rivers; Cole and Caraco, 2001). However, our results were comparable to the Chinese Rivers such as Yangtze (1297 ± 901 µatm; Wang et al., 2007), Pearl (450–2360 µatm; Zhang et al., 2007), Yellow (1137 ± 189 µatm; Cole and Caraco, 2001), and other Asian river such as Mekong (703–1475 µatm, Alin et al., 2011; 1090 ± 290 µatm; unpublished), and other world Rivers, i.e., Hudson (1125 ± 403 µatm, Raymond et al., 1997), St. Lawrence (1300 µatm, Helli et al., 2002), Ottawa rivers (1200 µatm, Telmer and Veizer, 1999) and Mississippi (1335 ± 130 µatm, Dubois et al., 2010).

Our areal flux of CO_2 in the river downstream the dam was intermediate relative to rivers in China (Table 5). For example, the CO_2 emission rate in the river downstream the Danjiangkou Reservoir was 8 times higher than that in the main channel of the Yangtze (ca.$14\,mmol\,m^{-2}\,d^{-2}$), while it was much lower with respect to the river reach

BGD
10, 10055–10094, 2013

downstream the dams in the Maotiao River (ca. 489 mmol m^{-2} d^{-2}) and the Xijiang (ca. 274 mmol m^{-2} d^{-2}). When compared to the world rivers, the estimated CO_2 emission flux per unit area was much lower than those in tropic rivers (e.g., Amazon), while was intermediate between those of temperate rivers and comparable to the global average (e.g., 147 mmol m^{-2} d^{-2}).

Similar to other reservoirs in China, downstream waters had quite high flux of CO_2 (cf. Yu et al., 2008; Wang et al., 2011). This could be explained as follows: turbines for hydroelectricity generation are located in the deep water areas, and this deep water with prevailing respiration property shows very high dissolved CO_2 concentration due to low permeability light and thermocline in particular. For example, CO_2 flux in the reservoir downstream was 13 fold that from reservoir surface in the Danjiangkou, and this could reach as high as 15 for Hongjiadu (Yu et al., 2008) and 33 for Hongfeng (Wang et al., 2011) (see Table 5). This suggested deep water releases via turbines is an important sources of atmospheric CO_2 (cf. Kemenes et al., 2011).

5 Conclusions

CO_2 outgassing flux across water–air interface in the Danjiangkou Reservoir was 1/13 lower than the flux from the river downstream the dam. Average CO_2 flux and annual CO_2 emission from the Reservoir were 9 mmol m^{-2} d^{-1} and 3.4×10^9 mol C yr^{-1}, respectively. CO_2 flux from the Danjiangkou Reservoir was near the lower end of the ranges from hydroelectric reservoirs in China, clearly lower than other global estimates for reservoirs (e.g., St Louis et al., 2000; McCully, 2006; Aufdenkampe et al., 2011) and natural lakes (Barros et al., 2011), while similar to global average for temperate hydroelectric reservoirs estimated by Barros et al. (2011).

Substantially monthly and spatial variations in pCO_2 and CO_2 flux demonstrated the dominant control of rainfall events particularly in the monsoon seasons, while biologic CO_2 uptake through aquatic photosynthesis dominated the spatial distributions in the reservoir area. The much higher CO_2 flux in the river downstream the reservoir was due

BGD
10, 10055–10094, 2013

to deep water releasing for power generation. Similar to other hydroelectric reservoirs in China, reservoir surface waters were generally supersaturated with CO_2 relative to atmosphere, while lower values of pCO_2 than the atmospheric level of CO_2 often occurred in the concentrated rainfall months and dry season. We concluded remarkably spatiotemporal variability in pCO_2 and CO_2 fluxes from China's reservoirs are urgently included for a substantial revision of global estimate of carbon emission, and water discharge from reservoirs should deserve extra attention for assessment of reservoirs' source and sink effects on atmospheric CO_2.

Supplementary material related to this article is available online at: http://www.biogeosciences-discuss.net/10/10055/2013/bgd-10-10055-2013-supplement.pdf.

Acknowledgements. The research is funded by the National Natural Science Foundation of China (No. 31100347, and No. 31130010), Youth Innovation Promotion Association, the Chinese Academy of Sciences, China.

References

Alin, S. R., Rasera, M. F. F. L., Salimon, C. I., Richey, J. E., Krusche, A. V., Holtgrieve, G. W., and Snidvongs, A.: Physical controls on carbon dioxide transfer velocity and flux in low-gradient river systems and implications for regional carbon budgets, J. Geophys. Res., 116, G01009, doi:10.1029/2010JG001398, 2011.

Amiotte Suchet, P., Probst, J. L., and Ludwig, W.: Worldwide distribution of continental rock lithology: implications for the atmospheric/soil CO_2 uptake by continental weathering and alkalinity river transport to the oceans, Global Biogeochem. Cy., 17, 1038, doi:10.1029/2002GB001891, 2003.

Aucour, A. M., Sheppard, S. M. F., Guyomar, O., and Wattelet, J.: Use of ^{13}C to trace origin and cycling of inorganic carbon in the Rhône River system, Chem. Geol., 159, 87–105, 1999.

BGD
10, 10055–10094, 2013

Aufdenkampe, A. K., Mayorga, E., Raymond, P. A., Melack, J. M., Doney, S. C., Alin, S. R., Aalto, R. E., and Yoo, K.: Riverine coupling of biogeochemical cycles between land, oceans, and atmosphere, Front. Ecol. Environ., 9, 53–60, 2011.

Barros, N., Cole, J. J., Tranvik, L. J., Prairie, Y. T., Bastviken, D., Huszar, V. L. M., del Giorgio, P., and Roland, F.: Carbon emission from hydroelectric reservoirs linked to reservoir age and latitude, Nat. Geosci., 4, 593–596, 2011.

Bastviken, D., Tranvik, L. J., Downing, J. A., Crill, P. M., and Enrich-Prast, A.: Freshwater methane emissions offset the continental carbon sink, Science, 331, 6013, doi:10.1126/science.1196808, 2011.

Butman, D. and Raymond, P. A.: Significant efflux of carbon dioxide from streams and rivers in the United States, Nat. Geosci., 4, 839–842, 2011.

Battin, T. J., Luyssaert, S., Kaplan, L. A., Aufdenkampe, A. K., Richter, A., and Tranvik, L. J.: The boundless carbon cycle, Nat. Geosci., 2, 598–600, 2009.

Chen, H., Wu, Y. Y., Yuan, X. Z., Gao, Y. S., Wu, N., and Zhu, D.: Methane emissions from newly created marshes in the drawdown area of the Three Gorges Reservoir, J. Geophys. Res., 114, D18301, doi:10.1029/2009JD012410, 2009.

Chen, H., Yuan, X. Z., Chen, Z. L., Wu, Y. Y., Liu, X. S., Zhu, D., Wu, N., Zhu, Q., Peng, C. H., and Li, W. Z.: Methane emissions from the surface of the Three Gorges Reservoir, J. Geophys. Res., 116, D21306, doi:10.1029/2011JD016244, 2011.

Chen, H., Zhu, Q., Peng, C. H., Wu, N., Wang, Y. F., Fang, X. Q., Hong, J., Xiang, W. H., Chang, J., Deng, X. W., and Yu, G. R.: Methane emissions from rice paddies natural wetlands, lakes in china: synthesis new estimate, Glob. Change Biol., 19, 19–32, 2013.

CSEPB (Chinese State Environment Protection Bureau): Water and Wastewater Monitoring Analysis Methods, 4th edn., Chinese Environment Science Press, Beijing, China, 2002 (in Chinese).

Cole, J. J. and Caraco, N. F.: Atmospheric exchange of carbon dioxide in a low-wind oligotrophic lake measured by the addition of SF6, Limnol. Oceanogr., 43, 647–656, 1998.

Cole, J. J. and Caraco, N. F.: Carbon in catchments: connecting terrestrial carbon losses with aquatic metabolism, Mar. Freshw. Res., 52, 101–110, 2001.

Cole, J. J., Caraco, N. F., and Peierls, B.L: Can phytoplankton maintain a positive carbon balance in a turbid, freshwater, tidal estuary, Limnol. Oceanogr., 37, 1608–1617, 1992.

Cole, J. J., Prairie, Y. T., Caraco, N. F., McDowell, W. H., Tranvik, L. J., Striegl, R. G., Duarte, C. M., Kortelainen, P., Downing, J. A., Middelburg, J. J., and Melack, J.: Plumbing the

BGD
10, 10055–10094, 2013

global carbon cycle: integrating Inland Waters into the terrestrial carbon budget, Ecosystems, 10, 171–184, 2007.
Dubois, K. D., Lee, D., and Veizer, J.: Isotopic constraints on alkalinity, dissolved organic carbon, and atmospheric carbon dioxide fluxes in the Mississippi River, J. Geophys. Res., 115, G02018, doi:10.1029/2009JG001102, 2010.
Dos Santos, M. A., Rosa, L. P., Sikar, B., Sikar, E., and Dos Santos, E. O.: Gross greenhouse gas fluxes from hydro-power reservoir compared to thermo-power plants, Energ. Policy, 34, 481–488, 2006.
Fearnside, P. M.: Hydroelectric dams in the Brazilian Amazon as sources of greenhouse gases, Environ. Conserv., 22, 7–19, 1995.
Fearnside, P. M.: Do hydroelectric dams mitigate global warming? The case of Brazil's CuruAuna Dam, Mitig. Adapt. Strat. Glob. Change, 10, 675–691, 2005.
Fearnside, P. M. and Pueyo, S.: Greenhouse-gas emissions from tropical dams, Nat. Clim. Change, 2, 382–384, 2012.
Giles. J.: Methane quashes green credentials of hydropower, Nature, 444, 524–525, 2006.
Guerin, F. and Abril, G.: Significance of pelagic aerobic methane oxidation in the methane and carbon budget of a tropical reservoir, J. Geophys. Res., 112, G03006, doi:10.1029/2006JG000393, 2007.
Guerin, F., Abril, G., Richard, S., Burban, B., Reynouard, C., Seyler, P., and Delmas, R.: Methane and carbon dioxide emissions from tropical reservoirs: significance of downstream rivers, Geophys. Res. Lett., 33, L21407, doi:10.1029/2006GL027929, 2006.
Hélie, J. F., Hillaire-Marcel, C., and Rondeau, B.: Seasonal changes in the sources and fluxes of dissolved inorganic carbon through the St. Lawrence River-isotopic and chemical constraint, Chem. Geol., 186, 117–138, 2002
Ho, D. T., Bliven, L. F., Wanninkhof, R., and Schlosser, P.: The effect of rain on air–water gas exchange, Tellus B, 49, 149–158, 1997.
Hope, D., Dawson, J. J. C., Cresser, M. S., and Billett, M. F.: A method for measuring free CO_2 in upland streamwater using headspace analysis, J. Hydrol., 166, 1–14, 1995.
Hunt, C. W., Salisbury, J. E., and Vandemark, D.: Contribution of non-carbonate anions to total alkalinity and overestimation of pCO_2 in New England and New Brunswick rivers, Biogeosciences, 8, 3069–3076, doi:10.5194/bg-8-3069-2011, 2011.
Huttunen, J. T., Väisänen, T. S., Hellsten, S. K., Heikkinen, M., Nykänen, H., Jungner, H., Niskanen, A., Virtanen, M. O., Lindqvist, O. V., Nenonen, O. S., and Martikainen, P. J.: Fluxes of

BGD
10, 10055–10094, 2013

CH_4, CO_2, and N_2O in hydroelectric reservoirs Lokka and Porttipahta in the northern boreal zone in Finland, Global Biogeochem. Cy., 16, 1003, doi:10.1029/2000GB001316, 2002.
Kemenes, M., Forsberg, B. R., and Melack, J. M.: Methane release below a tropical hydroelectric dam, Geophys. Res. Lett., 34, L12809, doi:10.1029/2007GL029479, 2007.
Kemenes, M., Forsberg, B. R., and Melack, J. M.: CO_2 emissions from a tropical hydroelectric reservoir (Balbina, Brazil), J. Geophys. Res., 116, G03004, doi:10.1029/2010JG001465, 2011.
Lewis, E. and Wallace, D. W. R.: Program Developed for CO_2 System Calculations, ORNL/CDIAC-105, Carbon Dioxide Information Analysis Center, Oak Ridge National Laboratory, US Department of Energy, Oak Ridge, TN, 1998.
Li, S. Y. and Lu, X. X.: Uncertainties of carbon emission from hydroelectric reservoirs, Nat. Hazards, 62, 1343–1345, 2012.
Li, S. Y. and Zhang, Q.: Geochemistry of the upper Han River basin, China, 1: Spatial distribution of major ion compositions and their controlling factors, Appl. Geochem., 23, 3535–3544, 2008.
Li, S. Y. and Zhang, Q.: Geochemistry of the upper Han River basin, China. 2: Seasonal variations in major ion compositions and contribution of precipitation chemistry to the dissolved load, J. Hazard. Mater., 170, 605–611, 2009.
Li, S. Y. and Zhang, Q.: Major ion chemistry and weathering processes of the Danjiangkou Reservoir, China, Hydrolog. Sci. J., 55, 1385–1395, 2010.
Li, S. Y., Gu, S., Liu, W., Han, H., and Zhang, Q.: Water quality in relation to the land use and land cover in the Upper Han River basin, China, Catena, 75, 216–222, 2008a.
Li, S. Y., Xu, Z., Cheng, X., and Zhang, Q.: Dissolved trace elements and heavy metals in the Danjiangkou Reservoir, China, Environ. Geol., 55, 977–983, 2008b
Li, S. Y., Cheng, X., Xu, Z., and Zhang, Q.: Spatial and temporal patterns of the water quality in the Danjiangkou Reservoir, China, Hydrolog. Sci. J., 54, 124–134, 2009a.
Li, S. Y., Liu, W., Gu, S., Cheng, X., Xu, Z., and Zhang, Q.: Spatio-temporal dynamics of nutrients in the upper Han River basin, China, J. Hazard. Mater., 162, 1340–1346, 2009b.
Li, S. Y., Xu, Z., Wang, H., Wang, J., and Zhang, Q.: Geochemistry of the upper Han River basin, China, 3: Anthropogenic inputs and chemical weathering to the dissolved load, Chem. Geol., 264, 89–95, 2009c.

BGD
10, 10055–10094, 2013

Li, S. Y., Lu, X. X., He, M., Zhou, Y., Li, L., and Ziegler, A. D.: Daily CO_2 partial pressure and CO_2 outgassing in the upper Yangtze River basin: a case study of the Longchuan River, China, J. Hydrol., 466–467, 141–150, 2012.

Li, S. Y., Xia, X., Tan, X., and Zhang, Q.: Effects of catchment and riparian landscape setting on water chemistry and seasonal evolution of water quality in the Upper Han River Basin, China, PLoS ONE, 8, e53163, 1–14, 2013.

Lima, I., Ramos, F., Bambace, L., and Rosa, R.: Methane emissions from large dams as renewable energy resources: a developing nation perspective, Mitigation and Adaptation Strategies for Global Change, 13, 193–206, 2008.

Lu, D. K., Yu, H. X., Ma, C. X., and Huang, P. W.: The correlation analysis between CO_2 at the water–air interface and environment factors in the Nihe Reservoir, Wetland Sci. Manag., 6, 44–48, 2010 (in Chinese with English abstract).

Mei, H. Y., Wang, F. S., Yao, C. Z., and Wang, B. L.: Diffusion flux of partial pressure of dissolved carbon dioxide in Wan'an reservoir in spring, Environm. Sci., 32, 58–63, 2011 (in Chinese with English abstract).

McCully, P.: Fizzy Science: Loosening the Hydro Industry's Grip on Reservoir Greenhouse Gas Emissions Research, International Rivers Network, 2006.

Neal, C., House, W. A., and Down, K.: An assessment of excess carbon dioxide partial pressures in natural waters based on pH and alkalinity measurements, Sci. Total Environ., 210/211, 173–185, 1998a.

Neal, C., House, W. A., Jarvie, H. P., and Eatherall, A.: The significance of dissolved carbon dioxide in major lowland rivers entering the North Sea, Sci. Total Environ., 210/211, 187–203, 1998b.

Qiu, J.: Chinese dam may be a methane menace, Nature, 29 Sept., doi:10.1038/news.2009.1962, 2009.

Raymond, P. A. and Cole, J. J.: Gas exchange in rivers and estuaries: choosing a gas transfer velocity, Estuaries, 24, 312–317, 2001.

Raymond, P. A., Caraco, N. F., and Cole, J. J.: Carbon dioxide concentration and atmospheric flux in the Hudson River, Estuaries, 20, 381–390, 1997.

Redfield, A. C.: The biological control of chemical factors in the environment, Am. Sci., 46, 205–221, 1958.

BGD
10, 10055–10094, 2013

Richey, J. E., Melack, J. M., Aufdenkampe, A. K., Ballester, V. M., and Hess, L. L.: Outgassing from Amazonian rivers and wetlands as a large tropical source of atmospheric CO_2, Nature, 416, 617–620, 2002.

Rosa, L. P., dos Santos, M. A., Matvienko, B., dos Santos, E. O., and Sikar, E.: Greenhouse gas emissions from hydroelectric reservoirs in tropical regions, Climatic Change, 66, 9–21, 2004.

Saito, L., Johnson, B. M., Bartholow, J., and Hanna, R. B.: Assessing ecosystem effects of reservoir operations using food web-energy transfer and water quality models, Ecosystems, 4, 105–125, 2001.

Sarma, V. V. S. S., Gupta, S. N. M., Babu, P. V. R., Acharya, T., Harikrishnachari, N., Vishnuvardhan, K., Rao, N. S., Reddy, N. P. C., Sarma, V. V., Sadhuram, Y., Murty, T. V. R., and Kumar, M. D.: Influence of river discharge on plankton metabolic rates in the tropical monsoon driven Godavari estuary, India, Estuar. Coast. Shelf S., 85, 515–524, 2009.

Sarma, V. V. S. S., Kumar, N. A., Prasad, V. R., Venkataramana, V., Appalanaidu, S., Sridevi, B., Kumar, B. S. K., Bharati, M. D., Subbaiah, C. V., Acharyya, T., Rao, G. D., Viswanadham, R., Gawade. L., Manjary, D. T., Kumar, P. P., Rajeev, K., Reddy, N. P. C., Sarma, V. V., Kumar, M. D., Sadhuram, Y., and Murty, T. V. R.: High CO_2 emissions from the tropical Godavari estuary (India) associated with monsoon river discharges, Geophys. Res. Lett., 38, L08601, doi:10.1029/2011GL046928, 2011.

St. Louis, V. L., Kelly, C. A., Duchemin, E., Rudd, J. W. M., and Rosenberg, D. M.: Reservoir surface as sources of greenhouse gases to the atmosphere: a global estimate, Bioscience, 50, 766–775, 2000.

Telmer, K. and Veizer, J.: Carbon fluxes, pCO_2 and substrate weathering in a large northern river basin, Canada: carbon isotope perspectives, Chem. Geol., 159, 61–86, 1999.

Teodoru, C. R., del Giorgio, P. A., Prairie, Y. T., and Camire, M.: Patterns in pCO_2 in boreal streams and rivers of northern Quebec, Canada, Global Biogeochem. Cy., 23, GB2012, doi:10.1029/2008GB003404, 2009.

Tranvik, L. J., Downing, J. A., Cotner, J. B., Loiselle, S. A., Striegl, R. G., Ballatore, T. G., Dillon, P., Finlay, K., Fortino, K., Knoll, L. B., Kortelainen, P. L., Kutser, T., Larsen, S., Laurion, I., Leech, D. M., McCallister, S. L., McKnight, D. M., Melack, J. M., Overholt, E., Porter, J. A., Prairie, Y., Renwick, W. H., Roland, F., Sherman, B. S., Schindler, D. W., Sobek, S., Tremblay, A., Vanni, M. J., Verschoor, A. M., Wachenfeldt, E., and Weyhenmeyer, G. A.: Lakes and

BGD
10, 10055–10094, 2013

reservoirs as regulators of carbon cycling and climate, Limnol. Oceanogr., 54, 2298–2314, 2009.
Wang, F. S., Wang, B. L., Liu, C. Q., Wang, Y. C., Guan, J., Liu, X. L., and Yu, X. L.: Carbon dioxide emission from surface water in cascade reservoirs-river system on the Maotiao River, southwest of China, Atmos. Environ., 45, 3827–3834, 2011.
Wang, F., Wang, Y., Zhang, J., Xu, H., and Wei, X.: Human impact on the historical change of CO_2 degassing flux in River Changjiang, Geochem. T., 8, 7, doi:10.1186/1467-4866-8-7, 2007.
Wanninkhof, R.: Relationship between wind speed and gas exchange over the ocean, J. Geophys. Res., 97, 7373–7382, 1992.
Yang, C., Telmer, K., and Veizer, J.: Chemical dynamics of the "St. Lawrence" riverine system: $\delta^{18}OH_2O$, $\delta^{13}CDIC$, $\delta^{34}S$ sulfate and dissolved $^{13}C/^{86}Sr$, Geochim. Cosmochim. Ac., 60, 851–866, 1996.
Yang, L., Lu, F., Wang, X. K., Duan, X. N., Song, W. Z., Sun, B. F., Chen, S., Zhang, Q. Q., Hou, P. Q., Zheng, F. X., Zhang, Y., Zhou, X. P., Zhou, Y. J., and Ouyang, Z. Y.: Surface methane emissions from different land use types during various water levels in three major drawdown areas of the Three Gorges Reservoir, J. Geophys. Res.-Atmos., 117, D10109, doi:10.1029/2011JD017362, 2012.
Yang, M., Li, H. L., Lei, T., Zhou, Y., Lu, C., Li, L., Lei, G. C., Wang, J. S., and Lu, X. G.: Spatial-temporal characteristics of methane emission flux and its influence factors at Minyun Reservoir in Beijing, Wetland Sci., 9, 191–197, 2011 (in Chinese with English abstract).
Yao, C. C., Wang, F. S., Wu, Y. Y., and Xu, H.: The vernal distribution of dissolved carbon dioxide (pCO_2) in the Xin'anjiang reservoir, J. Earth Environ., 1, 150–156, 2010 (in Chinese with English abstract).
Yao, G. R., Gao, Q. Z., Wang, Z. G., Huang, X. K., He, T., Zhang, Y. L., Jiao, S., and Ding, J.: Dynamics of CO_2 partial pressure and CO_2 outgassing in the lower reaches of the Xijiang River, a subtropical monsoon river in China, Sci. Total Environ., 376, 255–266, 2007.
Yu, Y. X., Liu, C. Q., Wang, F. S., Wang, B. L., Wang, S. L., and Liu, F.: Spatiotemporal characteristics and diffusion flux of partial pressure of dissolved carbon dioxide (pCO_2) in Hongjiadu reservoir, Chinese J. Ecol., 27, 1193–1199, 2008 (in Chinese with English abstract).
Zhai, W. D., Dai, M. H., and Guo, X. H.: Carbonate system and CO_2 degassing fluxes in the inner estuary of Changjiang (Yangtze) River, China, Mar. Chem., 107, 342–356, 2007.

BGD
10, 10055–10094, 2013

Zhang, S. R., Lu, X. X., Higgitt, D. L., Chen, C. T. A., Sun, H. G., and Han, J. T.: Water chemistry of the Zhujiang (Pearl River): natural processes and anthropogenic influences, J. Geophys. Res., 112, F01011, doi:10.1029/2006JF000493, 2007.

Zhao, D. Z., Tan, D. B., Wang, Z. H., and Li, Z.: Research on exchange law of CO_2 at water–air interface of Shuibuya Reservoir, Yangtze River, 8, 65–70, 2012 (in Chinese with English abstract).

Zhao, Y., Wu, B. F., and Zeng, Y.: Spatial and temporal patterns of greenhouse gas emissions from Three Gorges Reservoir of China, Biogeosciences, 10, 1219–1230, doi:10.5194/bg-10-1219-2013, 2013.

Zeng, F. W. and Masiello, C. A.: Sources of CO_2 evasion from two subtropical rivers in North America, Biogeochemistry, 100, 211–225, 2010.

Zheng, H., Zhao, X. J., Zhao, T. Q., Chen, F. L., Xu, W. H., Duan, X. N., Wang, X. K., and Ouyang, Z. Y.: Spatial-temporal variations of methane emissions from the Ertan hydroelectric reservoir in southwest China, Hydrol. Process., 25, 1391–1396, 2011.

BGD
10, 10055–10094, 2013

Table 1. The main features of the Danjiangkou Reservoir, China.

	Drainage area km^2	Height of dam m	Normal water level m	Total volume billion m^3	Water surface area km^2	Time of construction	Installed capacity M W	Power density $W m^{-2}$	Hydropower capacity 10^8 kWh yr^{-1}
1968–2013	95 200	162	157	17.45	745	1968	900	1.21	45
2014 afterward	95 200	176.6	172	29.05	1050	2014			

BGD
10, 10055–10094, 2013

Table 2. Descriptive statistics of monthly variability in T (°C), pH and alkalinity (μmol L^{-1}) of the Danjiangkou Reservoir, China.

	T					pH					Alkalinity				
	N	Mean	S.D.	Min.	Max.	N	Mean	S.D.	Min.	Max.	N	Mean	S.D.	Min.	Max.
Nov 2004	5	16.84	0.58	15.84	17.24	5	8.22	0.08	8.14	8.34	5	2440	219	2200	2600
Jan 2005	5	9.19	0.64	8.08	9.65	5	8.28	0.07	8.20	8.37	5	2360	207	2200	2700
Apr 2005	5	12.44	3.64	7.96	16.72	5	8.42	0.07	8.29	8.47	5	2600	524	2200	3500
Jun 2005	5	27.75	4.33	20.16	30.52	5	8.52	0.35	7.92	8.85	5	2409	291	1900	2643
Aug 2005	5	24.49	0.95	23.00	25.34	5	7.98	0.13	7.81	8.13	5	2180	192	1900	2400
Nov 2005	5	18.26	0.43	17.73	18.65	5	7.91	0.06	7.81	7.96	5	2280	286	1900	2600
Apr 2006	5	15.30	2.54	11.06	17.46	5	8.26	0.10	8.09	8.38	5	2432	489	2080	3280
Jul 2006	5	27.89	3.86	21.00	29.99	5	8.28	0.50	7.64	8.70	5	2192	485	1520	2880
May 2007	8	24.82	0.85	23.54	26.53	8	8.19	0.10	7.98	8.35	8	2520	363	2080	3280
Nov 2007	8	14.94	1.78	12.00	17.00										
Jul 2008	8	29.10	1.35	25.86	29.99	8	8.01	0.38	7.21	8.37	8	1937	345	1616	2644
Nov 2008	8	12.03	0.66	11.27	12.87	8	8.01	0.41	7.45	8.63	8	3241	332	2920	3968
Apr 2009	8	15.32	1.51	11.68	16.26	8	8.08	0.15	7.82	8.26	8	2489	384	2206	3422
Aug 2009	8	27.36	1.46	23.97	28.47	8	8.64	0.28	7.99	8.91	8	2037	222	1814	2359
Nov 2009	8	16.87	0.20	16.56	17.10	8	7.81	0.18	7.39	7.95	8	2354	151	2160	2576
Jan 2010	7	9.00	0.35	8.48	9.49	7	8.65	0.09	8.53	8.75	7	2354	166	2120	2560
Apr 2010	8	14.67	1.38	11.98	16.46	8	8.44	0.21	7.97	8.62	8	2409	226	2000	2680
Aug 2010											8	1795	456	1200	2360
Nov 2010											8	2475	92	2280	2600
Mar 2011											8	2407	257	2104	2736
May 2011	8	20.84	0.79	19.19	21.53	8	8.14	0.14	7.99	8.34	8	2717	226	2440	3000
Total	119	18.75	6.65	7.96	30.52	111	8.22	0.33	7.21	8.91	135	2385	425	1200	3968

S.D. – Standard deviation; Min. – Minimum; Max. – Maximum.

BGD
10, 10055–10094, 2013

Table 3. Descriptive statistics of spatial variability in T, pH and alkalinity of the Danjiangkou Reservoir, China (T in °C, Alkalinity in μmol L^{-1}).

		T					pH					Alkalinity				
		N	Mean	S.D.	Min.	Max.	N	Mean	S.D.	Min.	Max.	N	Mean	S.D.	Min.	Max.
Dan Reservoir	DJK1	17	20.45	6.49	9.26	30.52	16	8.15	0.27	7.76	8.62	19	2736	437	2000	3500
	DJK2	18	19.11	6.95	8.67	29.61	17	8.29	0.27	7.86	8.74	20	2473	292	2020	3360
	D3	10	18.97	6.96	8.85	29.53	9	8.26	0.36	7.68	8.79	12	2475	338	1960	3080
	DJK3	18	18.77	7.25	8.08	29.53	17	8.26	0.34	7.45	8.75	20	2444	284	1946	3120
Han Reservoir	DJK4	18	19.14	6.90	9.08	30.38	17	8.28	0.32	7.81	8.85	20	2117	390	1200	2960
	D2	10	18.68	6.88	9.23	29.66	9	8.31	0.34	7.80	8.91	12	2134	424	1280	2920
Dam	D3	10	18.61	6.85	9.18	29.91	9	8.28	0.35	7.78	8.82	12	2222	509	1320	3320
River downstream Dam	DJK5	18	16.39	5.82	7.96	25.86	17	8.01	0.38	7.21	8.64	20	2367	428	1951	3968
	Total	119	18.75	6.65	7.96	30.52	111	8.22	0.33	7.21	8.91	135	2385	425	1200	3968

S.D. – Standard deviation; Min. – Minimum; Max. – Maximum.

BGD
10, 10055–10094, 2013

Table 4. ANOVA for T, pH and alkalinity in month (a) and space (b) of the Danjiangkou Reservoir, China.

	(a) Month						(b) Space				
		Sum of Squares	df	Mean Square	F	p	Sum of Squares	df	Mean Square	F	p
T	Between Groups	4902	17	288	92.99	0.00	155	7	22	0.49	0.84
pH	Between Groups	7	16	0	7.52	0.00	1	7	0	1.49	0.18
Alkalinity	Between Groups	13 139 931	19	691 575	7.17	0.00	5 184 811	7	740 687	4.94	0.00
DIC	Between Groups	12 346 199	16	771 637	7.88	0.00	4 311 564	7	615 938	3.68	0.00
pCO_2	Between Groups	17 957 436	16	1 122 340	2.80	0.00	5 381 767	7	768 824	1.58	0.15
HCO_3^-	Between Groups	13 884 313	16	867 770	8.95	0.00	4 193 418	7	599 060	3.28	0.00
CO_3^{2-}	Between Groups	479 575	16	29 973	8.98	0.00	46 508	7	6644	0.92	0.50
CO_2	Between Groups	35 614	16	2226	3.45	0.00	7679	7	1097	1.28	0.27

BGD
10, 10055–10094, 2013

Table 5. Flux of CO_2 from the surface of rivers and reservoirs.

Name	Sites	Climate	FCO_2 mmol m^{-2} d^{-2}	References
Reservoirs				
Danjiangkou	**China**	**Subtropical**	**9**	**This study**
Three Gorges Reservoir	China	Subtropical	96	Zhao et al. (2013)
Three Gorges Reservoir (Xiangxi River)	China	Subtropical	42	Zhao et al. (2011)
Hongfeng	China	Subtropical	15	Wang et al. (2011)
Baihua	China	Subtropical	24	Wang et al. (2011)
Xiuwen	China	Subtropical	47	Wang et al. (2011)
Hongyan	China	Subtropical	22.4	Wang et al. (2011)
Hongjiadu	China	Subtropical	6.2	Yu et al. (2008)
Nihe	China	Subtropical	14.5	Lu et al. (2010)
Wan'an	China	Subtropical	12.8	Mei at al. (2011)
Xin'anjiang	China	Subtropical	7	Yao et al. (2010)
Shuibuya	China	Subtropical	18	Zhao et al. (2012)
Shasta		Temperate	28.3	Soumis et al. (2004)
Day Lake		Temperate	15.9	St. Louis et al. (2000)
Wallula		Temperate	−7.9	Soumis et al. (2004)
New Melones		Temperate	−27	Soumis et al. (2004)
Dworkshak		Temperate	−27.3	Soumis et al. (2004)
Arrow-Upper		Boreal	23.6	Tremblay et al. (2005)
La Grande 3		Boreal	38.8	Tremblay et al. (2005)
Lokka		Boreal	34.6	Huttunen et al. (2002)
Petit Saut		Tropic	133	Guerin et al. (2006)
Balbina		Tropic	76	Guerin et al. (2006)
Balbina		Tropic	314.7	Kemenes et al. (2007, 2011)
Samuel		Tropic	976	Guerin et al. (2006)
Tucurui		Tropic	308.3	St. Louis et al. (2000)
Tucurui		Tropic	181.8	Rosa et al. (2004)
Global Reservoirs		Temperate	31.8	St Louis et al. (2000)
Global Reservoirs		Temperate	12	McCully (2006)
Global Reservoirs		Temperate	8.8	Barros et al. (2011)
Global Reservoirs		Temperate	18.3	Aufdenkampe et al. (2011)
Global hydropower reservoirs			32.2	Barros et al. (2011)
Global artificial reservoirs			41.5	Barros et al. (2011)
Natural lakes			28.8	Barros et al. (2011)
Rivers				
River downstream the Dangjiangkou Reservoir		**Subtropical**	**119**	**This study**
Downstream the dams in the Maotiao		Subtropical	489	Wang et al. (2011)
Upstream the Wan'an Reservoir		Subtropical	210	Mei et al. (2011)
Downstream the Hongjiadu Reservoir		Subtropical	92.5	Yu et al. (2008)
Xijiang		Subtropical	274	Yao et al. (2007)
Changjiang		Subtropical	14.2	Wang et al. (2007)
Maotiao River in the Changjiang		Subtropical	362	Wang et al. (2011)
Longchuanjiang in the Changjiang		Subtropical	74	Li et al. (2012)
Amazon	Brazil	Tropic	189	Richey et al. (2002)
Amazon	Brazil	Tropic	345.2	Alin et al. (2011)
St.Lawrence	Canada	Temperate	78.1–294.5	Helli et al. (2001)
Ottawa	Canada	Temperate	80.8	Telmer and Veizer (1999)
Hudson	USA	Temperate	15.9–37	Raymond et al. (1997)
Mississippi		Temperate	269.9	Dubois et al. (2010)
USA rivers			202.7–915.1	Butman and Raymond (2011)
York River		Warm	22.7	Raymond and Bauer (2000)
Yukon		Boreal	171.2	Striegl et al. (2012)
Global rivers[a]			146.8	Cole et al. (2007)

[a] Carbon emission as CO_2 of 0.23 Pg yr^{-1} from Cole et al. (2007), river water surface water of 357 627 km^2 from Bastviken et al. (2011).

BGD
10, 10055–10094, 2013

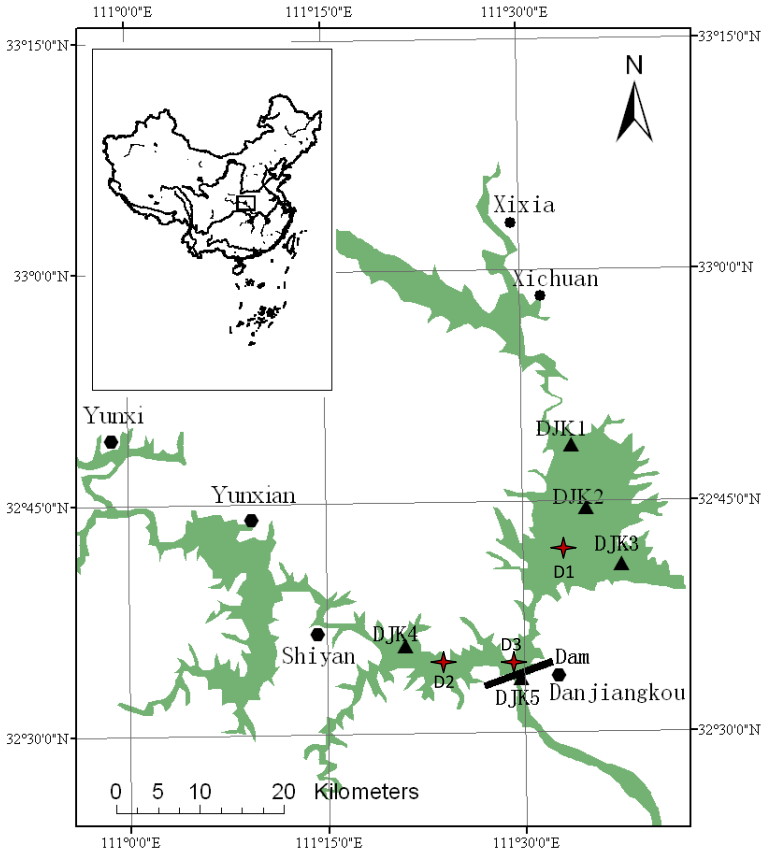

Fig. 1. Locations of eight sampling sites in the Danjiangkou Reservoir, China (DJK1, DJK2, D1 and DJK3 are located in the Dan Reservoir zone, DJK4 and D2 in the Han Reservoir zone, and D3 and DJK5 in the upstream and downstream of the dam, respectively. D1, D2 and D3 were added from 2007 afterward).

BGD
10, 10055–10094, 2013

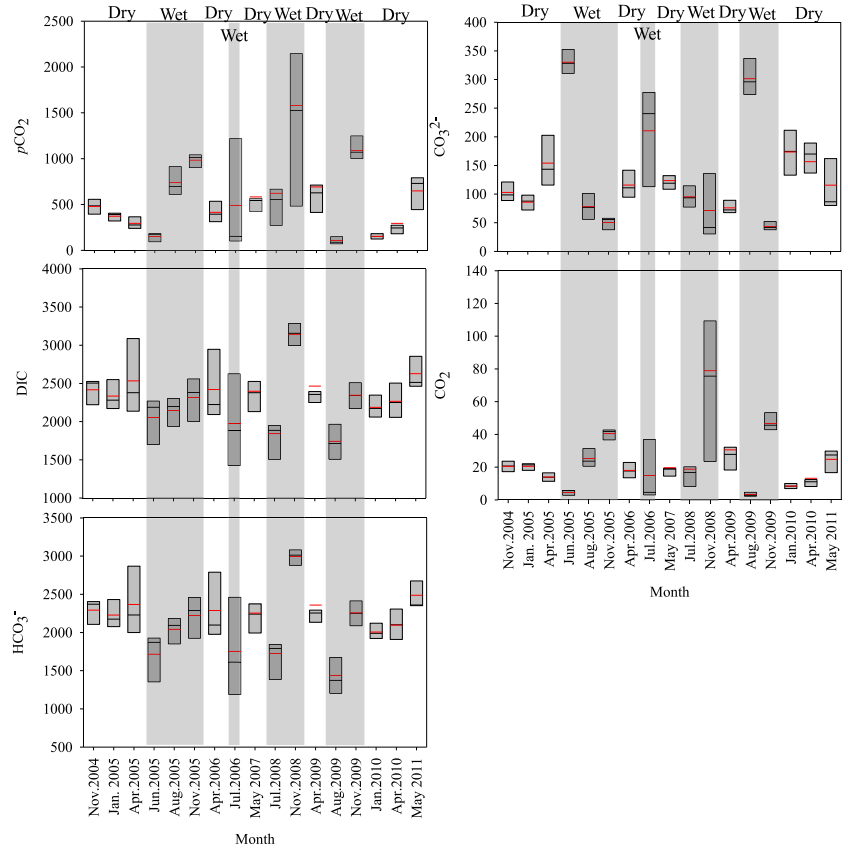

Fig. 2. Monthly DIC species illustrated by box-whiskers plots in the Danjiangkou Reservoir, China (the lower and upper boundary of a box represent the first (Q1) and the third quartile (Q3), respectively. The black and the red lines within the box represent the median and mean of the data set, respectively).

BGD
10, 10055–10094, 2013

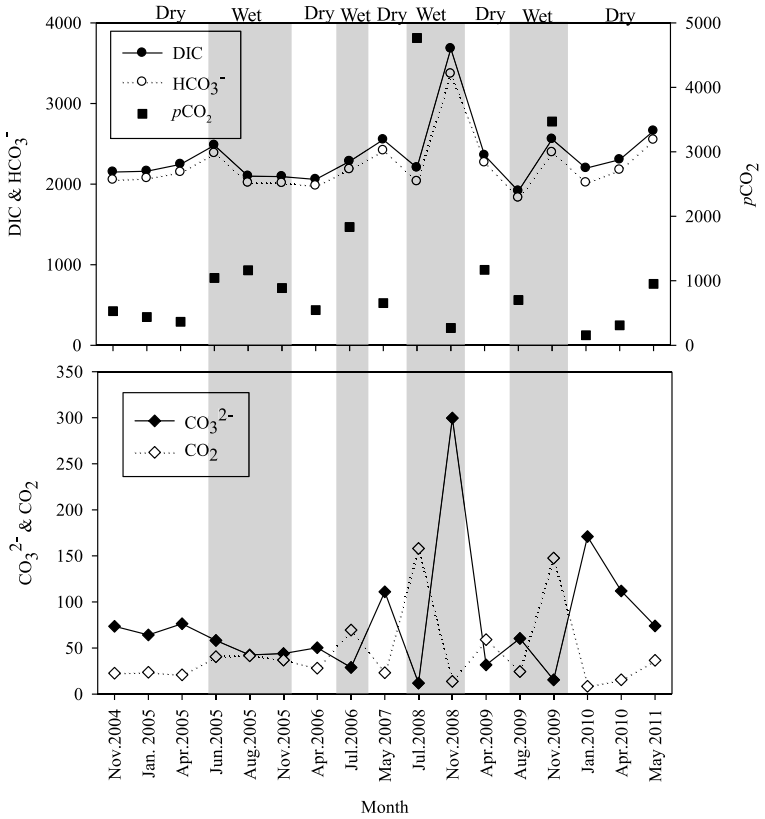

Fig. 3. Monthly DIC species in the river downstream the Danjiangkou Dam, China.

BGD
10, 10055–10094, 2013

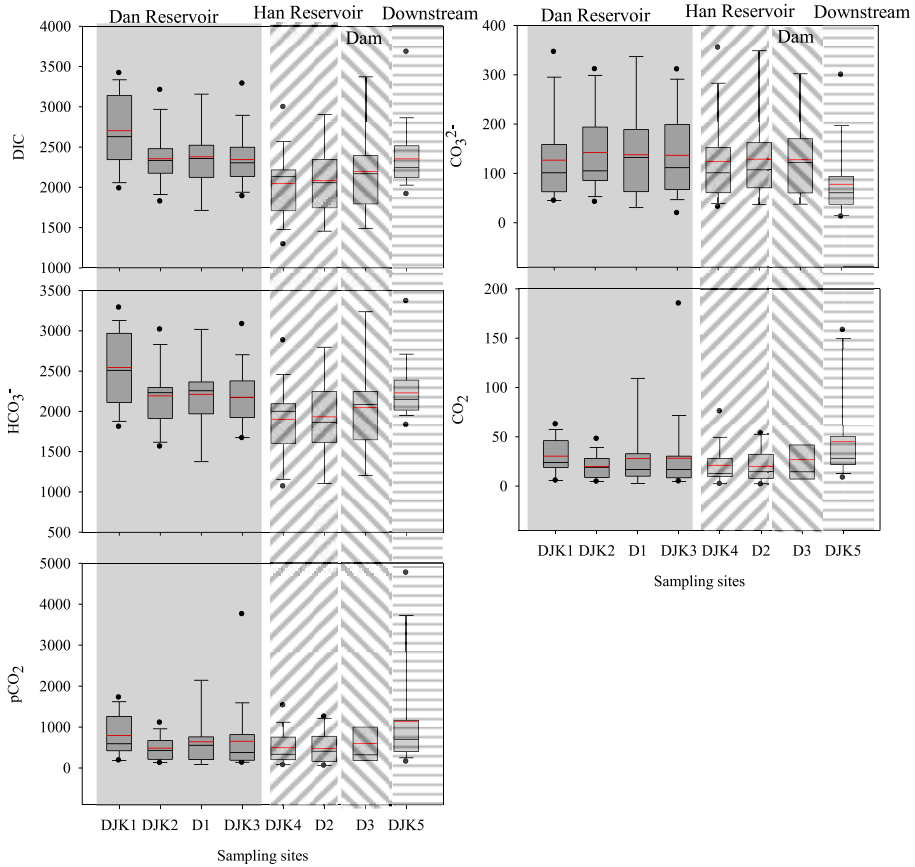

Fig. 4. Spatial variability in DIC species in the Danjiangkou Reservoir, China (box-whiskers plots, the black and red lines, lower and upper edges, bars and dots in or outside the boxes represent median and mean values, 25th and 75th, 5th and 95th, and < 5th and > 95th percentiles of all data, respectively).

BGD
10, 10055–10094, 2013

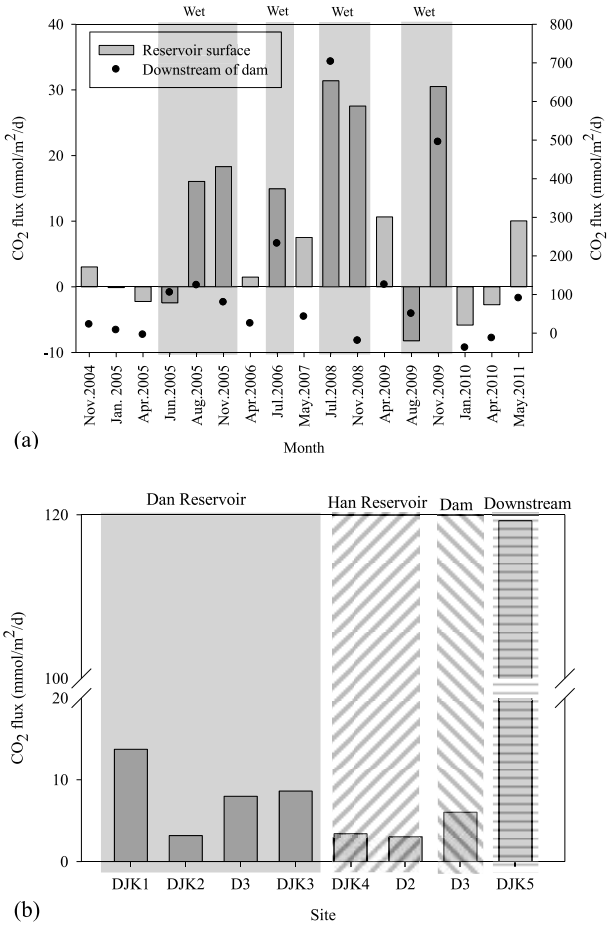

Fig. 5. Monthly **(a)** and spatial **(b)** variations of CO_2 diffusion fluxes in the Danjiangkou Reservoir, China.

BGD
10, 10055–10094, 2013

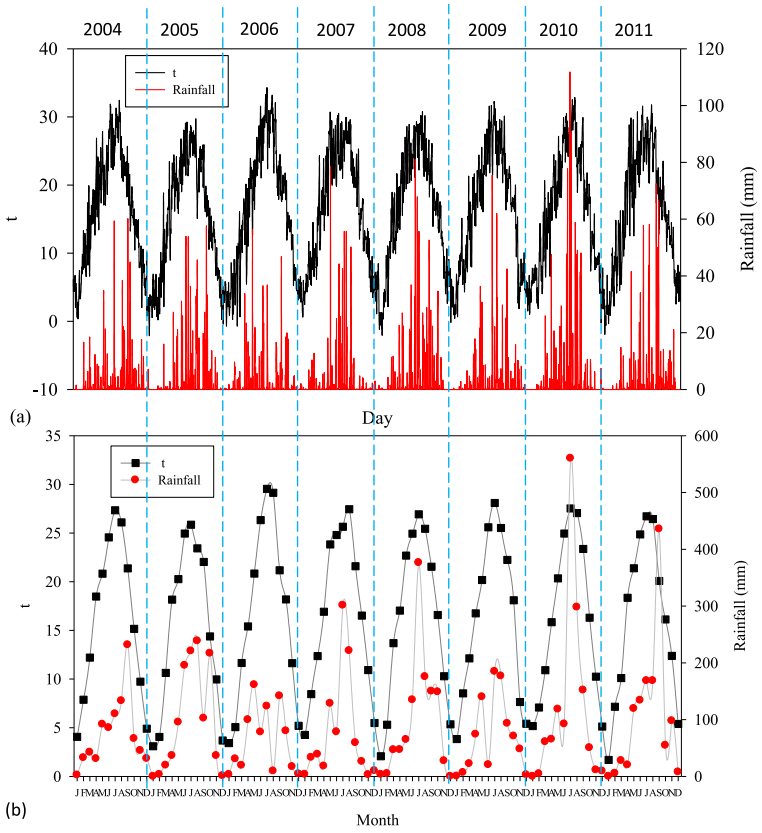

Fig. 6. Daily **(a)** and monthly **(b)** air temperature (°C) and rainfall (mm) in the upstream of the Danjiangkou Reservoir, China (Ankang station as an example, Ankang station is a most important station closest to the Reservoir; Data from NOAA).

BGD
10, 10055–10094, 2013

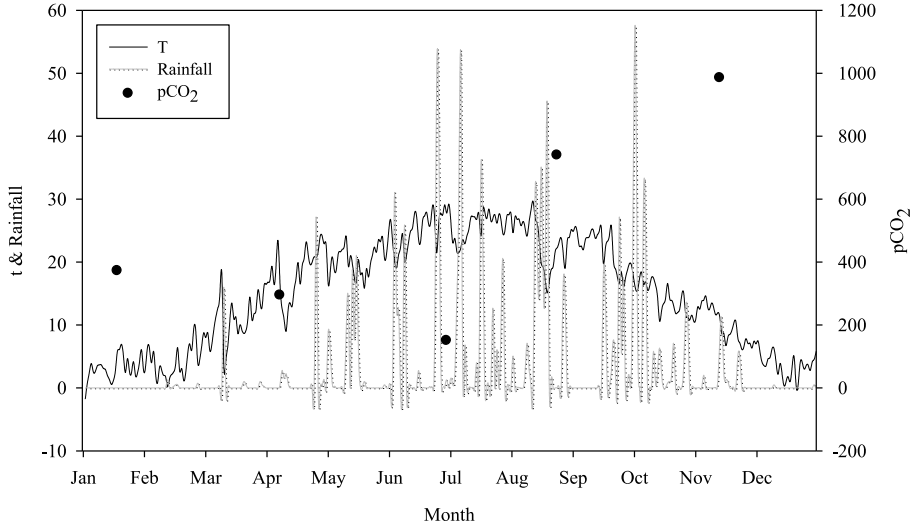

Fig. 7. Daily air temperature (°C), rainfall (mm) and pCO_2 (µatm) in the year 2005 of Ankang station.

BGD
10, 10055–10094, 2013

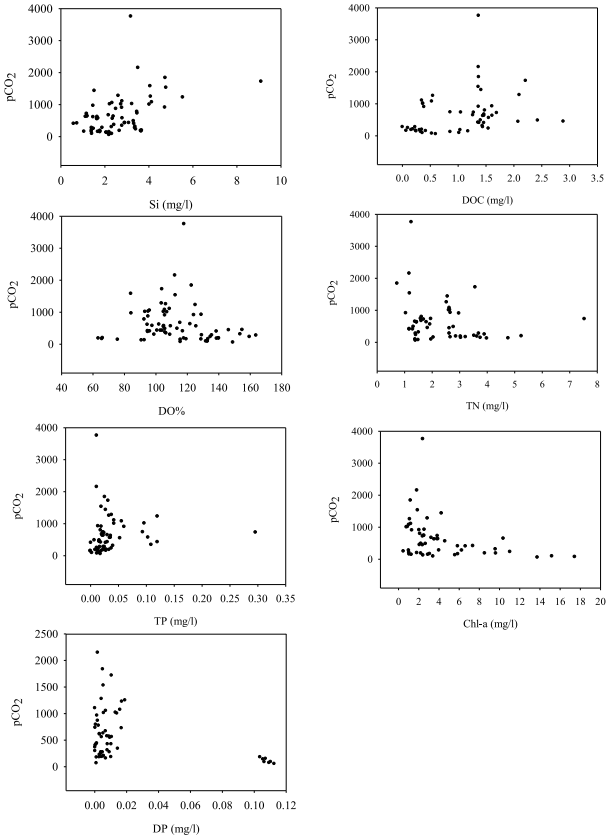

Fig. 8. Scatter plots between pCO_2 and some key water chemicals in the Danjiangkou Reservoir, China (Spearman's rho coefficients for pCO_2 and all the hydrogeochemical variables were tabulated in Table S2).

BGD
10, 10055–10094, 2013